Influence of rate of loading on fracture energy and strain softening of concrete

E.Brühwiler & F.H.Wittmann
Swiss Federal Institute of Technology, Lausanne
K.Rokugo
Gifu University, Japan

1 INTRODUCTION

Some concrete structures can be subjected to high loading rates. Typical examples are a column hit by a lorry, a safety containment under impact by missiles or stress waves from explosions. Another type of high rate of loading is given by seismic loading conditions. On the other side, structures when subjected to deformations due to ground movements may be loaded at very low loading rates.

It is known for some time already that concrete properties depend on rate of loading. Important efforts have been undertaken to study the behaviour of concrete both theoretically and experimentally under these conditions [Plank (ed.) 1982, Mindess and Shah (ed.) 1986]. Experimental studies have shown that both the compressive and the tensile strength increase significantly as the rate of loading is increased [Plank (ed.) 1982]. However, the influence of rate of loading on fracture energy has not yet been studied in detail.

In order to describe the failure behaviour of concrete in a realistic way, concepts of fracture mechanics must be introduced in numerical analysis. Hillerborg and his cowokers [1983] developed the ficticious crack model to describe the cracking and in particular crack propagtion of concrete. The concept of this model is based on the specific fracture energy G_F and the strain softening behaviour of concrete.

The aim of this contribution is to report values for the fracture energy and the strain softening diagram with respect to different rates of loading as determined by three different testing methods. In order to get the strain softening diagram of the material, the measured load-displacement curves have been analysed by means of finite element modules. In this way it is possible to deduce material laws for application in computerized structural analysis.

2 EXPERIMENTS AND RESULTS

Three different test series have been carried out.

In series A, beams were tested in three-point bending mode [Wittmann et al. 1987a] according to the RILEM recommendation [1985]. Fig. 1a shows a schematic representation of the experimental set-up and dimensions of the beam are given. The tests were run in a deflection controlled way. Load and deflection were recorded.

Series B [Wittmann et al. 1987c] consisted in tests on compact tension (CT) specimens. Geometry and dimensions are given in Fig. 1b. The tests were carried out with a servo-controlled hydraulic jack and controlled by means of crack opening displacement. Besides the load, the displacement in the plane of the loading points was measured.

Wedge splitting tests on notched cubes (see Fig. 1c) were performed in series C. The principle of this new testing method consists in splitting a notched cube by means of a wedge pressed between ball bearings placed on the top of the cube (Fig. 2b). The test is controlled by measuring the crack opening displacement using a clip gauge. The specimen shape and the principle were first proposed by Linsbauer and Tschegg [1986]. The loading device is similar to the one used by Hillemeier and Hilsdorf [1977] for the determination of K_{IC} of hardened cement paste and the interface. In order to get stable, i.e. controlled tests also at high displacement rates, a relatively large notch had to be sawn as to reduce the ratio of the specimen stiffness to the testing machine stiffness. The ligament area was 75 x 200 mm^2.

From all three testing methods, the specific fracture energy G_F can be obtained from the area under the load-displacement/deflection diagram divided by the ligament area.

Aggregates consisting of rounded river gravel and sand, were graded in accordance to Swiss standards (SIA 162) for aggregate sizes between 0 and 16 mm. The water-cement ratio was 0.4, the cement content 350 kg/m^3 for series A and B. The corresponding values for series C were 0.5 and 325 kg/m^3 respectively.

For series A and B, the compressive strength as determined on cylinders was 43 MPa and the tensile strength was 5.0 MPA. Concrete of series C had a compressive strength of 39 MPa and a tensile strength of 4.3 MPa. The modulus of elasticity (in compression) was 30'500 MPa for all types of concrete.

After demoulding the specimens of all three test series were water cured until testing. The notches in the beams and in the cubes were sawn, whereas the notch of the CT-specimens was casted.

For the 3-point bending test, the quasi-static loading condition is described in the RILEM-recommendation [1985] as the time (30-60 seconds) from the beginning of the test up to the peak load. This condition was adopted for the two other testing methods. The quasi-static loading rate corresponds to a strain rate of about $2.5 \cdot 10^{-6}$ s^{-1} in the initial crack tip as was found by a rough estimation. For reasons of comparison the relative rate defined as the ratio between the actual and the quasi-static rate was introduced. The wedge splitting test (series C) could be carried out under controlled conditions at a highest relative rate of $5 \cdot 10^3$. For this loading rate, a strain rate of 10^{-2} s^{-1} has been found by a rough estimation in the initial crack tip. This strain rate is in the upper range of earthquake loading rates. The lowest rate of $7.5 \cdot 10^{-3}$ was chosen in series A for the bending beams. The total duration of these tests was about 20 hours.

The relationship between the experimentally determined fracture energy and the loading rate can be described by equation (1). The parameters of this equation have been determined using a least squares fit. They are reported in Table I.

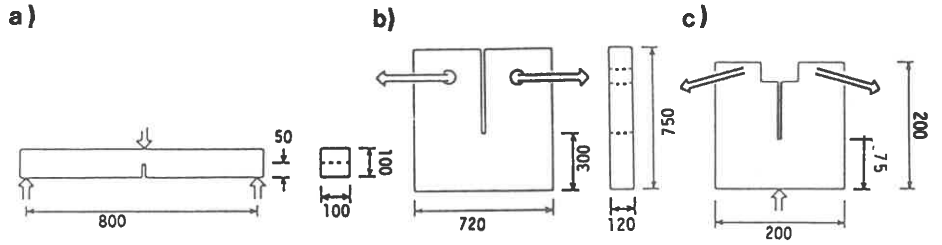

Figure 1. Three types of specimens : beam specimen (a); CT-specimen (b); wedge splitting cube (c).

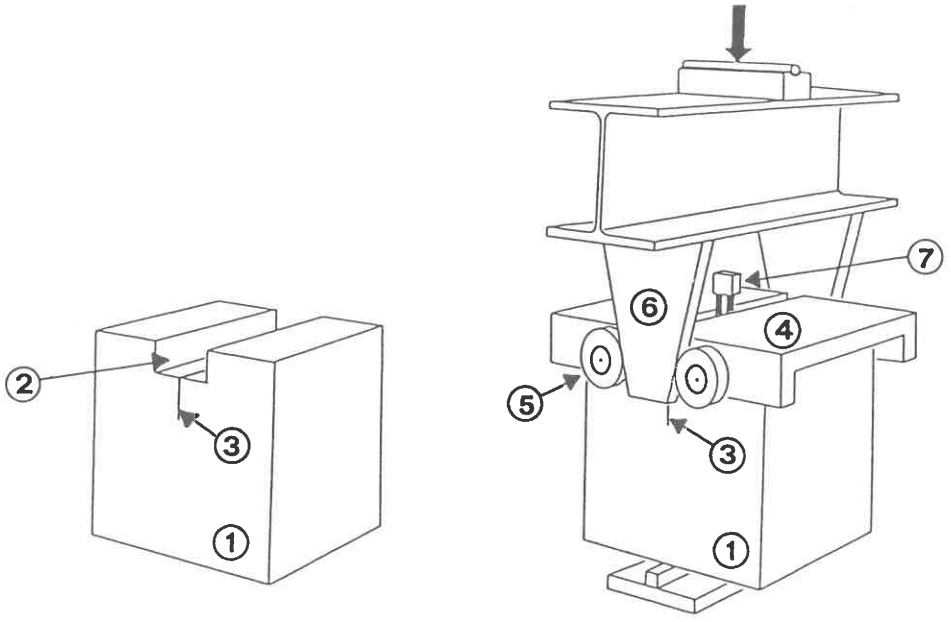

Figure 2. Wedge splitting test : test set-up (1 specimen; 2 groove; 3 notch; 4 loading device; 5 ball bearings; 6 wedge; 7 clip gauge).

Table 1. Parameters of equation (1) as determined with the three different test series.

	A	n	B	p	G_{FO} (N/m)
Series A	0.15	0.31	0.85	0.121	84
Series B	0.05	0.15	0.95	0.070	154
Series C	0.14	0.45	0.86	0.075	109

$$(1) \qquad \frac{G_F}{G_{FO}} = A \quad (\dot{v})^{-n} + B \ (\dot{v})^{p}$$

where $G_{FO} = G_F(\dot{v} = 1)$

$\dot{v}$: relative rate

A and B : constants

n and p : exponents

For high rates of loading equation (1) results in a power law. A stochastic approach has predicted a power law for the rate dependence of strength [Mihashi and Wittmann 1980]. The first term in this equation takes time-dependent processes such as creep into consideration.

The mean values of specific fracture energy G_F with respect to the relative rate are reported in Fig. 3.

It has been shown that the experimentally determined G_F-values depend on the ligament length [Wittmann et al. 1987c, Rokugo et al. 1987]. All values have been corrected and calculated for two different ligament lengths L_ℓ. In Fig. 3 the values obtained with the three different specimen geometries (beam, CT-specimen, and cube) are shown for a ligament length of L_ℓ = 50 mm and L_ℓ = 300 mm. The values plotted for L_ℓ = 300 mm are supposed to be independent of ligament length for large size specimen [Wittmann et al. 1987c, Rokugo et al. 1987].

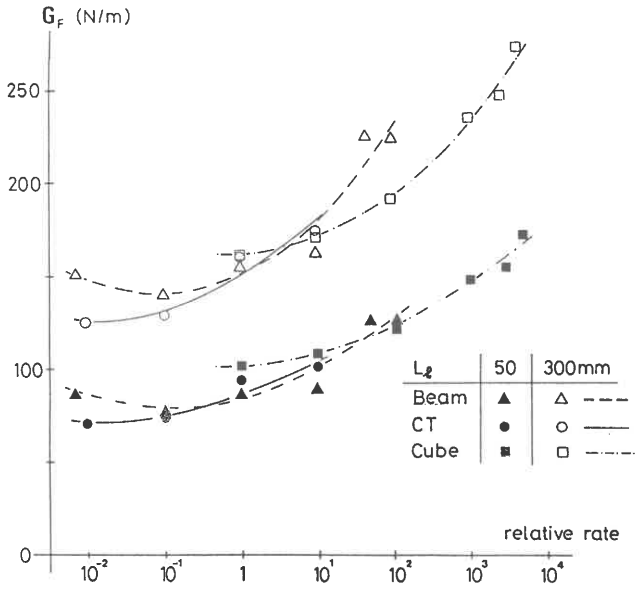

Figure 3. Effect of loading rate on fracture energy as determined for two different ligament lengths.

The mean load-displacement curves for four different relative rates from the wedge splitting test (series C) are shown in Fig. 4.

As has been shown in Fig. 3, fracture energy and hence the load-displacement curve are considerably influenced by the loading rate. In series C the fracture energy at the highest displacement rate is 70 % higher when compared to the quasi-static reference rate. The higher the displacement rate the stiffer the specimen and the higher the maximum load (Fig. 4). This increase of fracture energy at higher rates can be explained essentially by an increase of the tensile strength and the modulus of elasticity.

In series A the fracture energy passes through a minimum at intermediate rates. Fracture energy values at low rates may include some creep energy.

It has been shown that fracture energy alone is not sufficient for predictions of the real behaviour of concrete structures. The strain softening is needed in addition for computerized structural analysis. In order to obtain this relation, further numerical evaluation of the measured data is necessary.

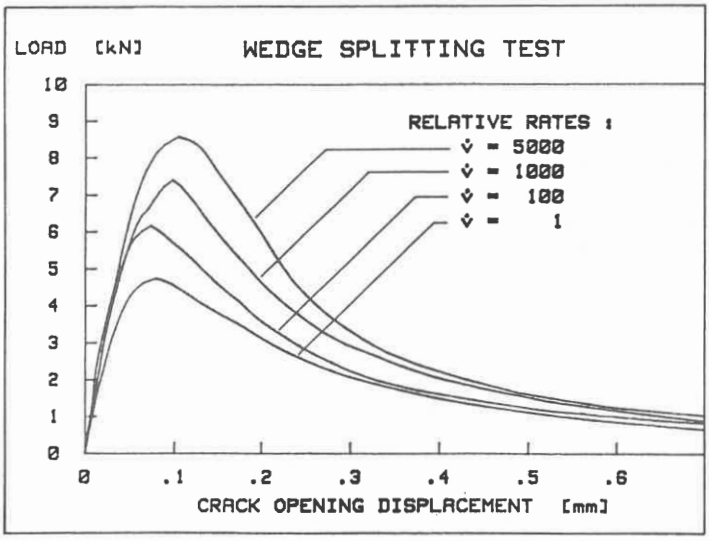

Figure 4. Load-crack opening displacement-diagrams (mean curves) from the wedge splitting tests (series C).

3. NUMERICAL EVALUATION OF MEASURED DATA

In order to obtain the tensile strain softening diagram, the measured load-displacement curves are analysed and numerically evaluated.

The module FRACTURE I [Roelfstra and Sadouki 1986] based on the finite element method and the ficticious crack model of Hillerborg [1983] has been developed to simulate crack formation and propagation in simple concrete elements such as the notched beam and the notched cube. By a special version called "SOFTFIT" the softening-diagram can be evaluated from measured load-displacement curves by a data fit [Roelfstra and Wittmann 1986].

In order to model the strain softening of the material, a bilinear relation has been chosen as a first approximation. The parameters of this bilinear strain softening diagram (Fig. 5a) are calculated by SOFTFIT as to obtain the best fitting load-displacement curve. In addition the fracture energy G_F is calculated from the area under the bilinear strain softening diagram.

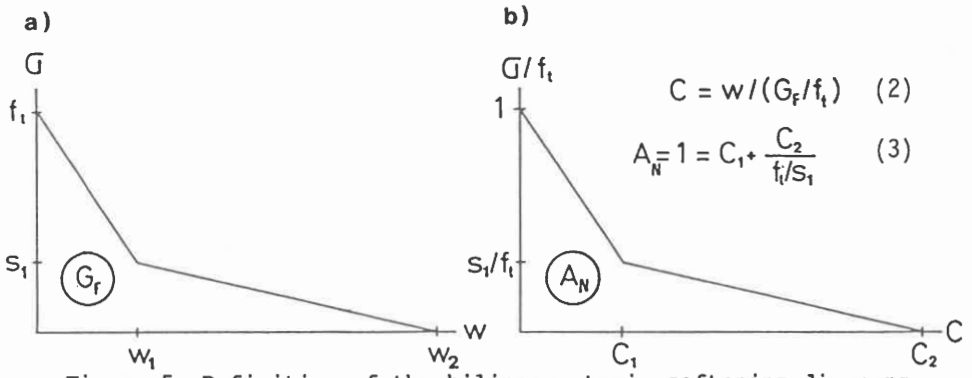

Figure 5. Definition of the bilinear strain softening diagrams
a) as used in the numerical analysis
b) normalized presentation

A parameter study showed that several bilinear diagrams can represent the real behaviour equally well [Rokugo et al. 1987]. Thus, additional assumptions have to be introduced as to obtain unique strain softening relations for the sake of comparative studies.

In this investigation, the tensile strength and the ration s_1/f_t have been fixed and the differences in both the maximum loads and square of the difference between the measured and simulated load-displacement curve were minimized. For the test series B (CT-tests), the tensile strength has been estimated based on the measured compressive strength and the maximum load observed for each rate. The ratio of f_t/s_1 was chosen to be 4. For the numerical evaluation of the wedge splitting tests, f_t for each rate was determined as the net bending strength using the maximum load. f_t/s_1 in this case was fixed to be 3. It should be mentioned here, that other ratios, for example f_t/s_1 = 2.5 or 5, would also lead to satisfying agreement.

In Fig. 6 experimentally determined load-displacement curves from the CT-tests are shown by a solid line with dots. The obtained curves from the data fit are introduced by a solid line. A good agreement between measured and calculated load-displacement curves can be observed. Moreover a good agreement between the G_F-values calculated from the softening-diagram and the G_F-values ad determined directly by means of the measured load-displacement diagram (solid lines with dots in Fig. 6) could be obtained.

In order to compare the shape of strain softening diagrams as determined under different test conditions, the calculated strain softening values are transformed into a normalized diagram (Fig. 5b). The stresses σ are related to the tensile strength f_t and the crack width w is represented by a constant C, defined in the following way :

(2) $\quad C = w / (G_F/f_t)$

The area A_N under the normalized bilinear strain softening diagram must be equal to 1 and can be expressed as follows :

$$(3) \qquad A_N = 1 = (C_1 + \frac{C_2}{f_t/s_1}) \cdot 0.5$$

The presentation of the strain softening values in a normalized diagram has the following aim. If the normalized strain softening diagrams show certain caracteristics for a given loading condition and concrete composition, the real strain softening diagram for different types of similar concretes and various specimens can be indicated without FE-analysis. They are then based exclusively on the corresponding f_t-value and the G_F-value as determined by independent measurements.

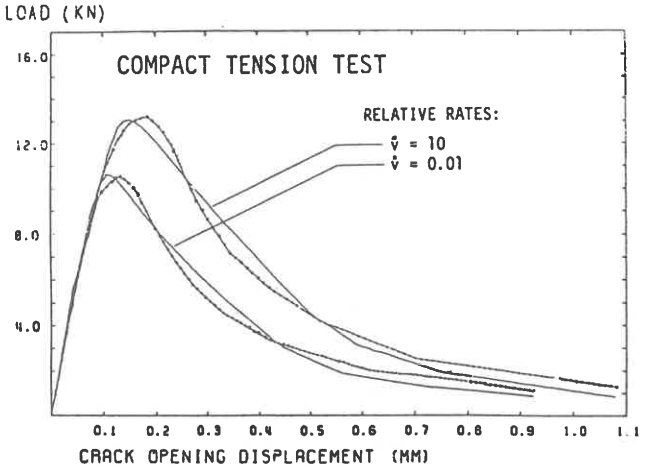

Figure 6. Comparison of measured (lines with dots) and fitted load-displacement curves from the CT-tests (series B).

The obtained normalized strain softening diagrams as evaluated from the test series B and C are reported in Fig. 7. The assumed tensile strength f_t and the calculated G_F-value are indicated in addition. It can be stated from Fig. 7 that for both series the normalized bilinear diagrams are all within a narrow band. They show no clear tendencies with respect to the investigated rates. Thus, the average normalized strain softening diagram, indicated by the mean c-values in Fig. 7, may be assumed to be independent of rate effects within the investigated range of loading rates.

The bilinear strain softening diagram as used in computerized structural analysis can be obtained with the help of the results given in the normalized presentation if in addition the rate dependent G_F- and f_t-values are known.

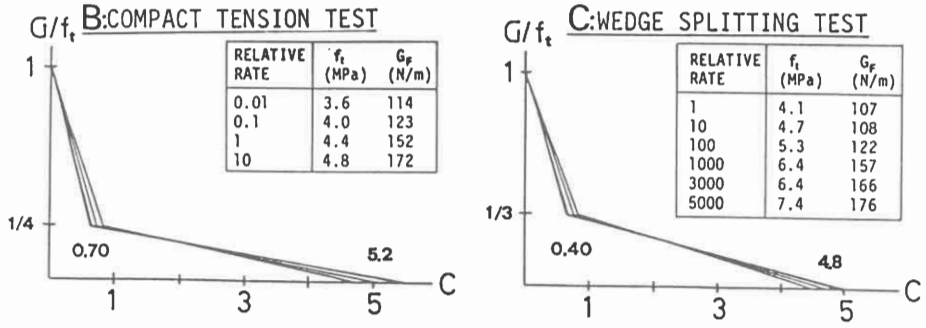

Figure 7. Normalized strain softening diagrams as determined from test series B and C.

4. CONCLUSIONS

1) The effect of loading rate on fracture mechanics parameters has been investigated by three different testing methods. The influence of the loading rate on the specific fracture energy G_F of concrete is significant. The G_F-value at a loading rate $5x10^3$ higher than static loading conditions increases by about 70 % as compared to the quasi-static G_F-value. At loading rates lower than the quasi-static one, the fracture energy tend to increase due to time-dependent processes such as damage due to microcracking and creep. Hence the fracture energy as a function of the loading rate passes through a minimum.

2) With the assumption of a bilinear strain softening diagram load-deflection curves as determined by the 3-point-bending test and load-displacement-curves measured by means of the CT-test and the wedge splitting test can be calculated numerically. The parameters of the strain softening diagram are then determined by data fitting. The G_F-values calculated from the softening-diagrams are in good agreement with the experimentally obtained fracture energy values.

3) For reasons of comparison the strain softening parameters are transformed into a normalized presentation. As the shapes of these normalized strain softening diagrams are not significantly affected by loading rate, one diagram may be used in a numerical analysis to describe the strain softening behaviour of concrete within the investigated rates. Only the rate dependent values for the tensile strength f_t and the specific fracture energy G_F for the corresponding concrete have to be known.

4) The bilinear strain softening relation must be considered to be a first, but simple approximation of the real function. As it leads to satisfying results in the numerical simulation of fracture mechanics tests, i.e. a good agreement between measured and calculated load-displacement curves, the concept of fracture energy may be applied in computerized structural analysis.

REFERENCES

Hillemeier, B. & H.K. Hilsdorf. 1977. Fracture mechanics studies on concrete compounds. Cement and Concrete Research, Vol. 7:523-536.

Hillerborg, A. 1983. Analysis of one single crack. F.H. Wittmann (ed.), Fracture mechanics of concrete, Elsevier:223-249.

Linsbauer, H. & E. Tschegg. 1986. Fracture energy determination of concrete with cube-shaped specimens. Zement und Beton 31 (Heft 1):38-40.

Mihashi, H. & F.H. Wittmann. 1980. Stochastic approach to study the influence of rate of loading on strength of concrete. Heron (The Netherlands) 25, No 3.

Mindess, S. & S.P. Shah (editors). 1986. Cement based composites : strain rate effects on fracture. MRS Symposium, MRS Pittsburgh, Vol. 64.

Plank, G. (editor). 1982. Concrete structures under impact and impulsive loading. Proceedings RILEM-CEB-IABSE-IASS-Interassociation Symposium, Bundesanstalt für Materialprüfung (BAM), Berlin.

RILEM-Draft-Recommendation (50-FMC). 1985. Determination of fracture energy of mortar and concrete by means of three-point bend test on notched beams. Materials and Structures, 18:285-290.

Roelfstra, P.E. & H. Sadouki. 1986. Fracture I, theory and applications. Laboratory for Building Materials, Swiss Federal Institute of Technology Lausanne.

Roelfstra, P.E. & F.H. Wittmann. 1986. Numerical method to link strain softening with failure of concrete. F.H. Wittmann (ed.), Fracture toughness and fracture energy of concrete. Elsevier:163-175.

Rokugo, K., E. Brühwiler, H. Mihashi & F.H. Wittmann. 1987. Methods to determine fracture energy and strain softening of concrete. Contribution to this volume.

Wittmann, F.H., Yiun-Yuang Huang, P.E. Roelfstra, H. Mihashi, N. Nomura & Xin-Hua Zhang. 1987a. Influence of age of loading, water-cement ratio and rate of loading on fracture energy of concrete. Materials and Structures. (To be published).

Wittmann, F.H., K. Rokugo, E. Brühwiler, H. Mihashi & Ph. Simonin. 1987c. Fracture energy and strain softening of concrete as determined by means of compact tension specimens. (Accepted for publication).